Improving the performances of current optical interferometers & future designs
Proceedings of Haute Provence Observatory Colloquium (23-27 September 2013)
Edited by L. Arnold, H. Le Coroller & J. Surdej

Imaging Young Stellar Objects with VLTi/PIONIER

J. Kluska[1], F. Malbet[1], J.-P. Berger[2], M. Benisty[1], B. Lazareff[1], J.-B. Le Bouquin[1], F. Baron[3], C. Dominik[4], A. Isella[5], A. Juhasz[6], S. Kraus[7], R. Lachaume[8], F. Ménard[1,9], R. Millan-Gabet[5], J. Monnier[10], C. Pinte[9], F. Soulez[11], M. Tallon[11], W.-F. Thi[1], É. Thiébaut[11] & G. Zins[1]

[1] *UJF-Grenoble 1 / CNRS-INSU, Institut de Planétologie et d'Astrophysique de Grenoble (IPAG) UMR 5274, Grenoble, F-38041, France*

[2] *ESO, Garching, Germany*

[3] *Georgia State University, Atlanta, USA*

[4] *University of Amsterdam, Amsterdam, The Netherlands*

[5] *California Institute of Technology, Pasadena, USA*

[6] *Leiden Observatory, Leiden, The Nertherlands*

[7] *University of Exeter, UK*

[8] *Pontificia Universidad Católica de Chile. Santiago de Chile, Chile*

[9] *UMI-FCA, CNRS y U. de Chile, Chile*

[10] *University of Michigan, Ann Arbor, USA*

[11] *Université de Lyon I, Lyon, France*

Abstract. Optical interferometry imaging is designed to help us to reveal complex astronomical sources without a prior model. Among these complex objects are the young stars and their environments, which have a typical morphology with a point-like source, surrounded by circumstellar material with unknown morphology. To image them, we have developed a numerical method that removes completely the stellar point source and reconstructs the rest of the image, using the differences in the spectral behavior between the star and its circumstellar material. We aim to reveal the first Astronomical Units of these objects where many physical phenomena could interplay: the

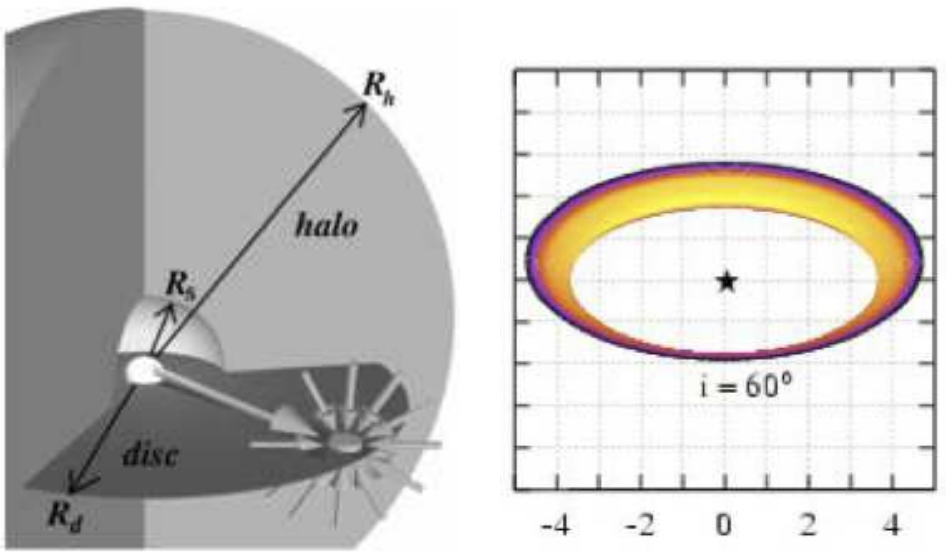

Figure 1.: *Left : Plot from Vinkovic et al. (2003) showing the halo scenario. Right : The puffed-up inner rim scenario proposed by Isella & Natta (2005).*

dust sublimation causing a puffed-up inner rim, a dusty halo, a dusty wind or an inner gaseous component. To investigate more deeply these regions, we carried out the first Large Program survey of HAeBe stars with two main goals: statistics on the geometry of these objects at the first astronomical unit scale and imaging their very close environment. The images reveal the environment, which is not polluted by the star and allows us to derive the best fit for the flux ratio and the spectral slope. We present the first images from this survey and the application of the imaging method on other astronomical objects.

1. Introduction

Direct imaging techniques have revealed complex structures around young stellar objects (e.g. Rameau et al. 2013) such as spirals, holes, etc. These features are the consequence of phenomena occurring more closer to the star, like planetary formation. To reach these regions we need more angular resolution. This is where optical interferometry is entering the game.

1.1 The inner regions of Young Stellar Objects (YSO).

The inner parts of the Young Stellar Objects are the place of many physical processes. In the near infrared, one of the most contributing phenomena (in the broad band) is the dust sublimation. Dust sublimates at 1500K which is the temperature of the dust at approximately 1 AU of its host star (for Herbig stars). It creates an excess emission in the near infrared but is not well constrain geometrically. Vinkovic et al. (2003) proposed a halo model to explain the excess

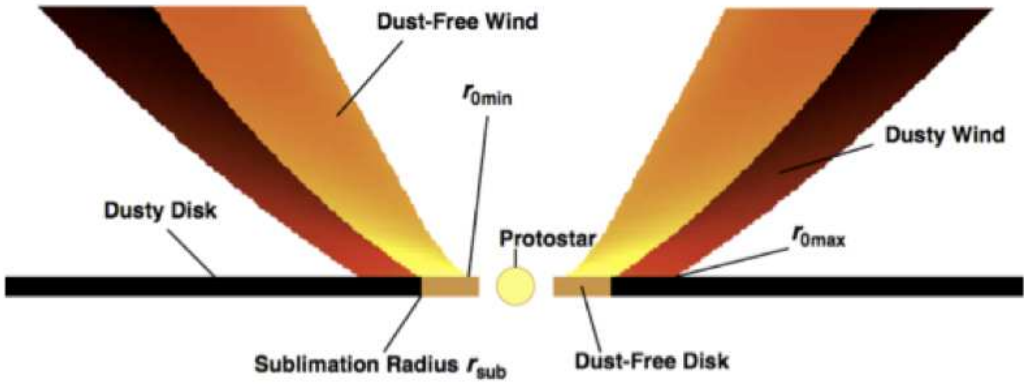

Figure 2.: *The disk wind solution proposed by Bans & Königl (2012).*

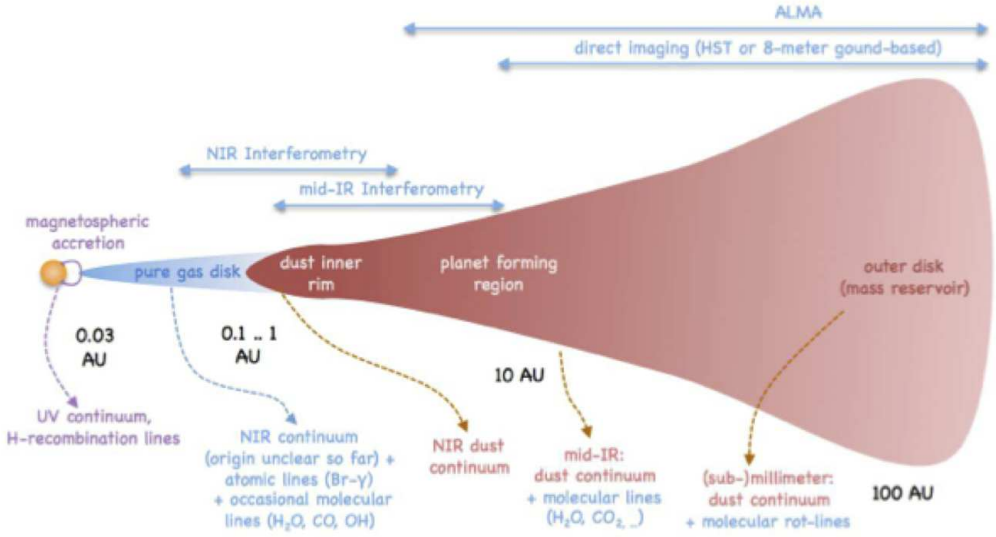

Figure 3.: *This is the sketch from Dullemond & Monnier (2010) of the inner regions of young stellar objects where we expect to see the dust sublimation region, an inner accretion disk and constrain the planetary formation.*

emission in the near infrared and Isella & Natta (2005) proposed a model of a puffed-up inner rim due to dust sublimation (see Fig. 1). More recently, Bans & Königl (2012) published a wind scenario to explain this excess and said that optical interferometry is the tool to distinguish between the scenarios (see Fig. 2).

In addition to dust sublimation, gas could create an accretion disk inside the dust sublimation radius and cause magneto-spheric accretion onto the star. Planetary formation could also perturb the inner rim. We can also expect mass ejection through wind and/or jets that are believed to originate in this inner region. A schematic view is displayed in Fig. 3.

In order to study this complex inner regions and being model independent, we want to make image reconstruction from optical interferometry data.

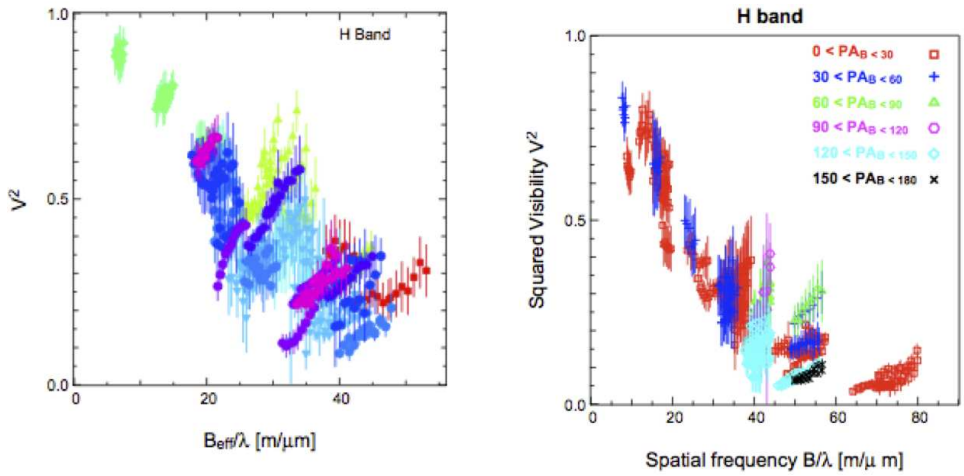

Figure 4.: *Datasets on YSOs obtained with AMBER. HR5999 data is from Benisty et al. (2011) and HD163296 data from Renard et al. (2010). We can clearly see the chromatic effect.*

1.2 YSO and chromatism

First reconstructed images of Young Stellar Objects (YSOs) have already been made. For instance Benisty et al. (2011) made an image of HR5999 and Renard et al. (2010) an image of HD163296. These images were obtain with monochromatic image reconstruction algorithms. As we can see on the visibility curves, there is a strong chromatic effect in particular in the H-band (see Fig. 4). The longest wavelengths have clearly lower visibilities than the shortest ones. It is an astrophysical effect.

Kluska et al. (2012) showed that if we are in a presence of an unresolved star which is in the Rayleigh-Jeans regime and a resolved environment which is cold ($\approx$ 1500K) we will have such an effect. In the near infrared, the young stellar objects SED is shared between the stellar photosphere flux and the environment one. The changing flux ratio between a resolved environment and a point source creates the chromatic effect seen in the squared visibilities seen in both AMBER (Petrov et al. 2007) and PIONIER (Le Bouquin et al. 2011) data.

2. Chromatic method to reconstruct on object

The monochromatic image reconstruction algorithms are not adapted anymore for such a chromaticity. To face this problem two approaches exist. The first one is a three dimensional approach that consists in reconstructing a spectral cube of images adding a trans-spectral regularization term (see Soulez et al.). Another approach, which will be presented here, is the Semi-Parametric Approach for image Reconstruction of Chromatic Objects (SPARCO : Kluska et al. 2014).

2.1 Flux parametrization

The chromatic effect needs to be taken into account in a chromatic algorithm. That is why we need to define the flux evolution of both the photosphere and the

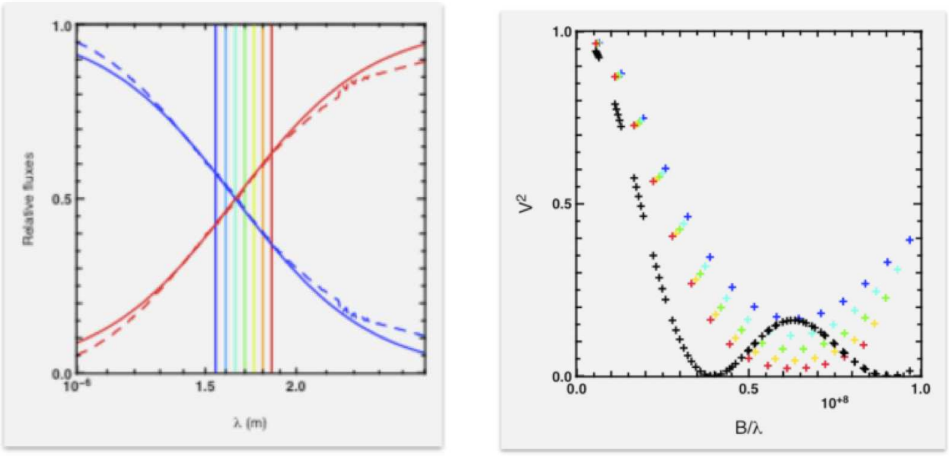

Figure 5.: *Left : fluxes versus wavelength across the H-band. In blue : flux of the photosphere. In red : the flux of the environment. In solid lines : the fluxes defined by Eq. 1. In dashed line : fluxes defined by a photosphere + environment model. Vertical color lines : PIONIER spectral channels. Right : squared visibilities from a ring alone (black) and a ring with a star (color).*

environment. As written in Sect.1.2, the photosphere is in the Rayleigh-Jeans regime and have its flux $F_\lambda \propto \lambda^{-4}$ (or a spectral index of -4). The environment flux could also be described as a power-law with a spectral index $d_{\rm env}$ (for 1500K $d_{\rm env} = 0.8$ for H-band). To define the total flux we need the fraction of flux of the star f_*^0 at λ_0 (which is an arbitrary chosen wavelength). We can then write the total flux $f_{tot}(\lambda)$ as :

$$f_{tot}(\lambda) = f_*^0 \left(\frac{\lambda}{\lambda_0}\right)^{-4} + (1 - f_*^0)\left(\frac{\lambda}{\lambda_0}\right)^{d_{\rm env}} \tag{1}$$

where first term is the stellar flux ($f_*(\lambda)$) and the second one is the flux of the environment ($f_{\rm env}$). This flux parametrization is valid in a narrow band such as the H-band (see Fig. 5, Left).

2.2 Visibility computation

With the fluxes definition, we can compute the total visibilities. To do so we need to set the visibilities for the star and the environment separately. For the photosphere we assume that it is not resolved and its visibility is $V_* = 1$. This assumption is valid considering that a $5R_\odot$ at 140pc (distance of the Taurus star forming region) has a visibility of 0.997 for B=100m in the H-band.

The visibility of the environment ($\widetilde{V}_{\rm env}$) will be computed from the image as it is done in monochromatic image reconstruction algorithms. The star is not appearing in the image anymore.

The equation of the total visibility that is fitted to the data is :

$$\widetilde{V}_{\rm tot}\left(\frac{\mathbf{b}}{\lambda}, \lambda\right) = \frac{f_*(\lambda) + f_{\rm env}(\lambda)\widetilde{V}_{\rm env}(\frac{\mathbf{b}}{\lambda})}{f_*(\lambda) + f_{\rm env}(\lambda)} \tag{2}$$

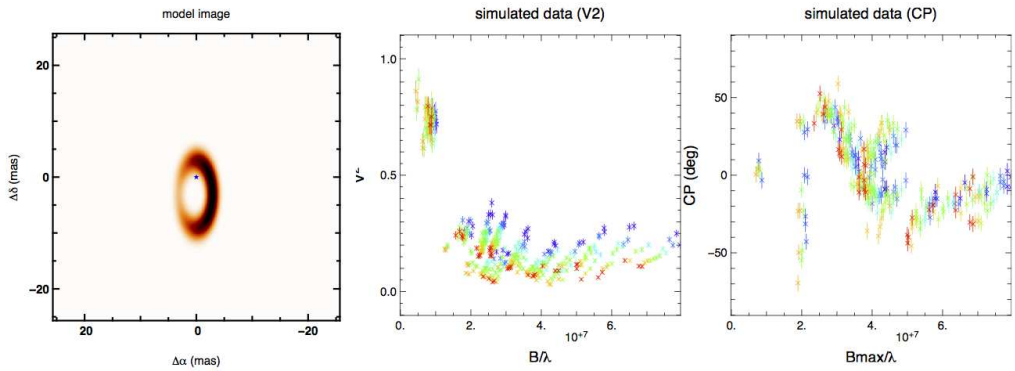

Figure 6.: *Left : The model image. The star is represented with a red star in the middle of the image. The ring is azimuthally modulated and shifted with respect to the star. Center and Right : squared visiblities and closure phases of the model taking a actual* (u, v)*-plan. A gaussian noise was added to this dataset. The colors represent the spectral channels as on the previous figures.*

where $(\frac{\mathbf{b}}{\lambda})$ is the spatial frequency (which is the baseline vector divided by the wavelength).

Thanks to the linearity of the Fourier transform we can separate the star from the image of the environment. The algorithm is described more specifically in Kluska et al. (2014). The result of a ring visibility taking into account the chromatic effect i shown Fig. 5 Right.

2.3 Validation on a model

The algorithm was tested on a chromatic model of a YSO. It is composed of a star, having 40% of the flux at 1.65μm. The environment is an azimuthally modulated gaussian ring, shifted to the south with respect to the star. The environmental spectral index is set to 1. The model image is showed in Fig. 6. In order to generate a realistic (u, v)-plan we have taken an existing one on an object already observed by PIONIER. The (u, v)-plan is then not totally optimal. We then generate the squared visibilities (V^2) and the closure phases (CP). The whole data set is shown in Fig. 6.

The image reconstructions are shown in Fig. 7. They were performed using the `MiRA` (Thiébaut 2008) algorithm. They were made using three methods :

- An image reconstruction with a monochromatic algorithm. The χ^2 is not satisfactory ($\approx$ 10). There are many artifacts in the image due to the chromaticity present in the data.
- An image reconstruction by subtracting the star from the image but without taking into account the chromaticity. The χ^2 is slightly better but the image is still not satisfactory.
- An image reconstruction applying the SPARCO method. This method was tested in both `MiRA` and `MACIM` (Ireland et al. 2006) algorithm with a $\chi^2 = 1.2$. The features of the ring are well retrieved and the artifacts are weak.

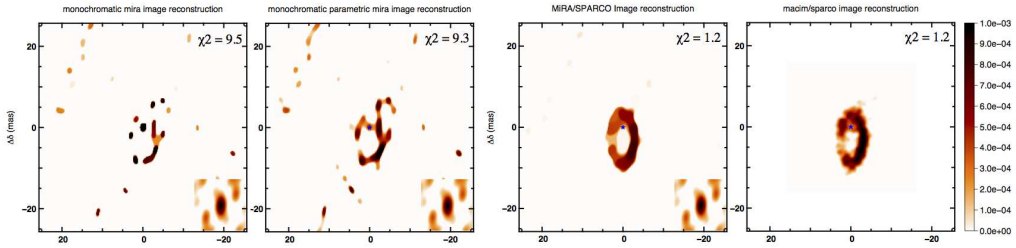

Figure 7.: *Image reconstructions on the model using different methods. Left : classical monochromatic image reconstruction. Center Left : monochromatic image reconstruction subtracting the star. Right : chromatic image reconstruction subtracting the star with* `Mira` *and* `MACIM`*. In the right bottom corner : the dirty beam of the* (u, v)*-plan.*

2.4 Chromatic degeneracy

The reconstructions showed in Sect. 2.3 were made setting the chromatic parameters f_*^0 and $d_{\rm env}$ to the right ones (0.4 and 1 respectively).

Without spectrophotometric informations we have no information on these chromatic parameters. What are the effects on the image reconstruction process if the chromatic parameters are wrong ? To test that, we have made a bunch of images that with different values of the chromatic parameters (see Fig. 8). The image with the good parameters is in the center. We have taken a range of spectral indexes for the environment that represent temperatures from 1250K to 1750K (spectral indexes of 2 and 0 respectively). For these temperatures the image does not vary much for a fixed value of the flux ratio. The effects are bigger for the flux ratios. If we put too much flux in the star (50% for instance) the image is filled by artifacts and the ring is dug. But if the stellar to total flux ratio is too low, some flux will be put at the position of the star degrading the quality of the image.

We can also make a χ^2-map of the imager reconstructions in the plan of the chromatic parameters. This map is presented in Fig. 9. We can see there is a smooth valley of χ^2 that indicates a clear degeneracy between the two chromatic parameters. The spectrophotometric data can be used to find the good values of the chromatic parameters.

3. Imaging real targets

Once the chromatic image reconstruction method is validated we have applied it on actual datasets. We have conducted a Large Program with the PIONIER instrument on the VLT interferometer. 55 Herbig Ae/Be stars were observed during our 30 nights of observation. A dozen of objects are resolved enough to be imaged. We present images made on two objects in Fig. 10.

These images were obtain by taking the chromatic parameters showing the minimum χ^2 value.

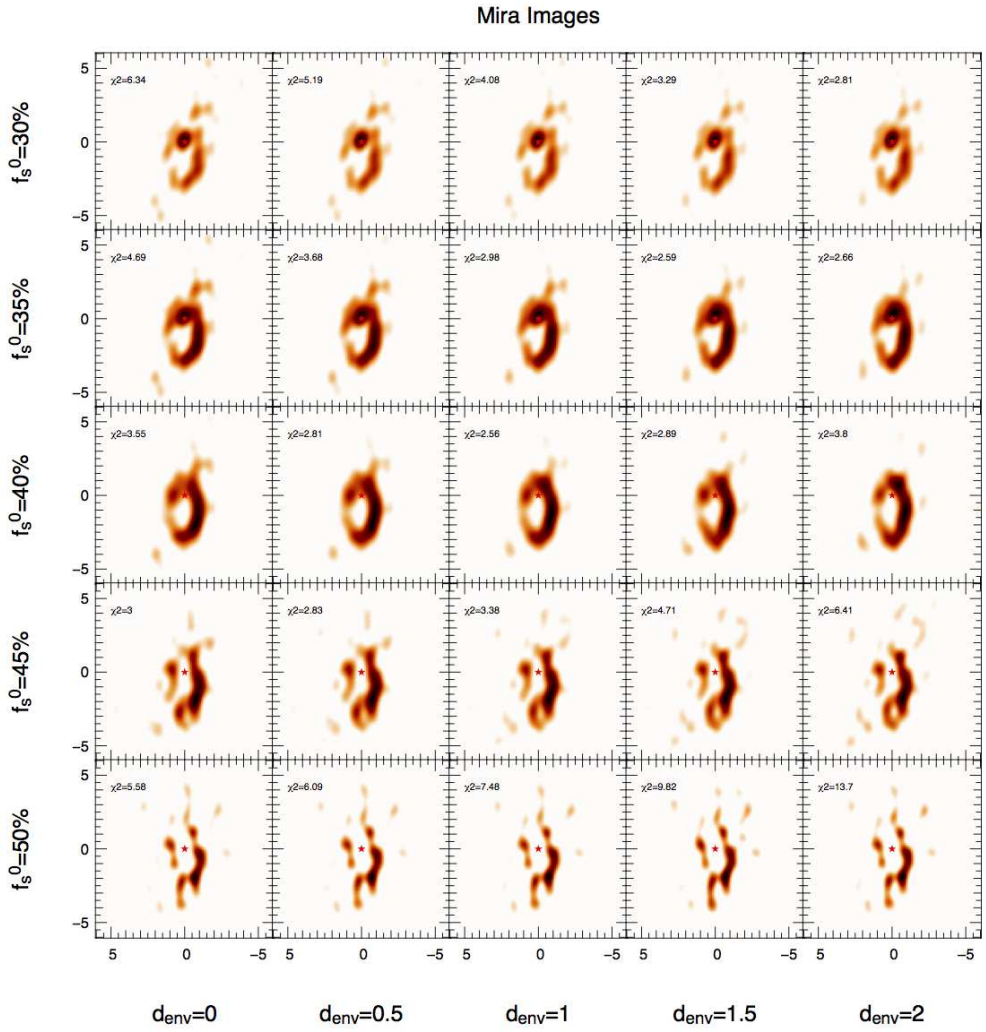

Figure 8.: *The mosaic of chromatic parameters. In the x-axis : the spectral index of the environment ($d_{\rm env}$). In the y-axis : the stellar to total flux ratio (f_*^0). The good values are in the center. We can see how an error on a chromatic parameter is affecting the image.*

HD45677 is a Be star which is well resolved for the interferometer. We can clearly see a ring like structure which is brightest in one of his sides. This is most easily interpreted as a inclination effect.

The second object, HD98922, is also a Be star, supposed to be very young. We can clearly see its ring in the image which can be interpreted as the dust sublimation ring.

These images are preliminary and have to be interpreted more precisely. But we can see that the image reconstruction method is able to retrieve a correct brightness distribution of these objects by assuming a correct value for the environment temperature.

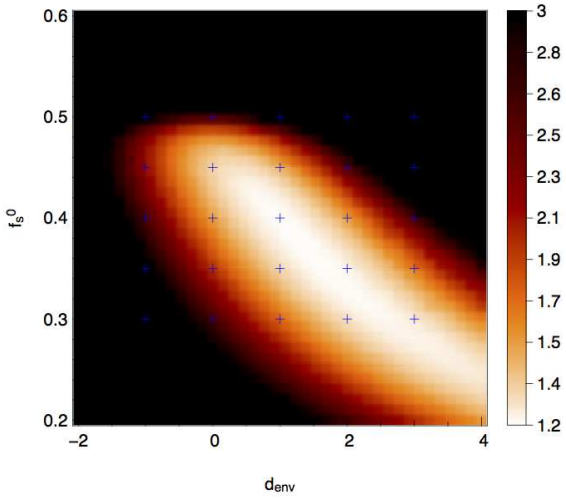

Figure 9.: *The χ^2-map in the space of the chromatic parameters. There is a clear χ^2-valley showing a degeneracy between the two parameters.*

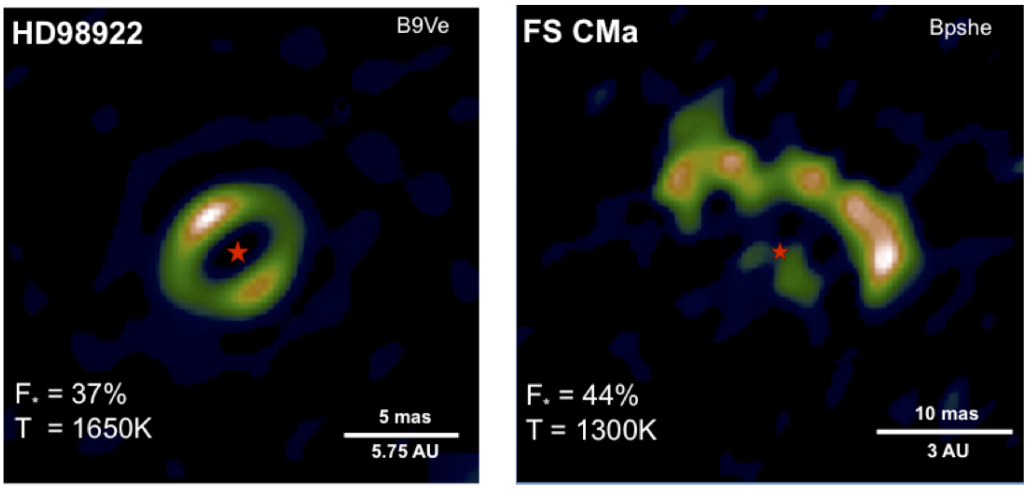

Figure 10.: *Left : an image reconstruction on HD98922. Right : an image reconstruction on HD45677*

4. Conclusion

We have presented a new method to perform image reconstructions that takes into account the chromaticity of Young Stellar Objects. To do so it introduces two chromatic parameters that are the stellar to total flux ratio and the spectral index of the environment. This technique is adapted to the case where the flux ratio between the star and its environment is changing across a bandwidth and if it is the main effect.

Nevertheless this method is showing a degeneracy showing a χ^2 valley in the chromatic parameter space. This is why spectro-photometric information is

necessary to precisely separate the flux of the star of the environment one and to correctly reconstruct the image.

We showed in the last section the ability of the method to reconstruct images on actual dataset gathered by PIONIER/VLTi on Herbig Ae/Be Stars.

This method can be applied on other astrophysical objects showing a unresolved and a resolved component with different temperatures such as planetary nebulae, AGB stars or Active Galactic Nuclei.

Acknowledgements. This work is supported by the French ANR POLCA project (Processing of pOLychromatic interferometriC data for Astrophysics, ANR-10-BLAN-0511).

References

Bans, A. and Königl, A., 2012, ApJ, 758, 100

Benisty, M., Renard, S., Natta, A., Berger, J.-P., Massi, F., Malbet, F., Garcia, P.-J.-V., Isella, A., Mérand, A., Monin, J.-L., Testi, L., Thiébaut, E., Vannier, M. & Weigelt, G., 2011, A&A, 531, A84

Dullemond, C. P. and Monnier, J. D., 2010, ARA&A, 48, 205

Ireland, M. J., Monnier, J. D. & Thureau, N., 2006, Society of Photo-Optical Instrumentation Engineers (SPIE) Conference Series, 6268, 58

Isella, A. and Natta, A., 2005, A&A, 438, 899

Kluska, J., Malbet, F., Berger, J.-P., Lazareff, B., Le Bouquin, J.-B., Benisty, M., Menard, F., Pinte, C. Millan-Gabet, R., & Traub, W., 2012, Society of Photo-Optical Instrumentation Engineers (SPIE) Conference Series, 8445, 0O

Kluska, J., Malbet, F., Berger, J.-P., Baron, F., Lazareff, B., Le Bouquin, J.-B., Monnier, J. D., Soulez, F. & Thiébaut. E., 2014, A&A, submitted.

Le Bouquin, J.-B., Berger, J.-P., Lazareff, B., Zins, G., Haguenauer, P., Jocou, L., Kern, P., Millan-Gabet, R., Traub, W., Absil, O., Augereau, J.-C., Benisty, M., Blind, N., Bonfils, X., Bourget, P., Delboulbe, A., Feautrier, P., Germain, M. and Gitton, P., Gillier, D., Kiekebusch, M., Kluska, J., Knudstrup, J., Labeye, P., Lizon, J.-L., Monin, J.-L., Magnard, Y., Malbet, F., Maurel, D., Ménard, F., Micallef, M., Michaud, L., Montagnier, G., Morel, S., Moulin, T., Perraut, K., Popovic, D., Rabou, P., Rochat, S., Rojas, C., Roussel, F., Roux, A., Stadler, E., Stefl, S., Tatulli, E. & Ventura, N., 2011, A&A, 535, A67

Petrov, R. G., Malbet, F., Weigelt, G., Antonelli, P., Beckmann, U., Bresson, Y., Chelli, A., Dugué, M., Duvert, G., Gennari, S., Glück, L., Kern, P., Lagarde, S., Le Coarer, E., Lisi, F., Millour, F., Perraut, K., Puget, P., Rantakyrö, F., Robbe-Dubois, S., Roussel, A., Salinari, P., Tatulli, E., Zins, G., Accardo, M., Acke, B., Agabi, K., Altariba, E., Arezki, B., Aristidi, E., Baffa, C., Behrend, J., Blöcker, T., Bonhomme, S., Busoni, S., Cassaing, F., Clausse, J.-M., Colin, J., Connot, C., Delboulbé, A., Domiciano de Souza, A., Driebe, T., Feautrier, P., Ferruzzi, D., Forveille, T., Fossat, E., Foy, R., Fraix-Burnet, D., Gallardo, A., Giani, E., Gil, C., Glentzlin, A., Heiden, M., Heininger, M., Hernandez Utrera, O., Hofmann, K.-H., Kamm, D., Kiekebusch, M., Kraus, S., Le Contel, D., Le

Contel, J.-M., Lesourd, T., Lopez, B., Lopez, M., Magnard, Y., Marconi, A., Mars, G., Martinot-Lagarde, G., Mathias, P., Mège, P., Monin, J.-L., Mouillet, D., Mourard, D., Nussbaum, E., Ohnaka, K., Pacheco, J., Perrier, C., Rabbia, Y., Rebattu, S., Reynaud, F., Richichi, A., Robini, A., Sacchettini, M., Schertl, D., Schöller, M., Solscheid, W., Spang, A., Stee, P., Stefanini, P., Tallon, M., Tallon-Bosc, I., Tasso, D., Testi, L., Vakili, F., von der Lühe, O., Valtier, J.-C., Vannier, M. & Ventura, N., 2007, A&A, 464, 1

Rameau, J., Chauvin, G., Lagrange, A.-M., Thébault, P., Milli, J., Girard, J. H. & Bonnefoy, M., 2012, A&A, 546, A24

Renard, S., Malbet, F., Benisty, M., Thiébaut, E. & Berger, J.-P., 2010, A&A, 519, A26

Thiébaut, E., 2008, Society of Photo-Optical Instrumentation Engineers (SPIE) Conference Series, 7013, 43

Vinković, D., Ivezić, Ž., Miroshnichenko, A. S. & Elitzur, M., 2003, MNRAS, 346, 1151